

Article

Interacting Multiple Model for Lithium-Ion Battery State of Charge Estimation Based on the Electrochemical Impedance Spectroscopy

Ce Huang ¹ , Haibin Wu ^{1,*} , Zhi Li ², Ran Li ² and Hui Sun ³ 

¹ Heilongjiang Province Key Laboratory of Laser Spectroscopy Technology and Application, School of Measurement and Communication Engineering, Harbin University of Science and Technology, Harbin 150080, China

² School of Electrical and Electronic Engineering, Harbin University of Science and Technology, Harbin 150080, China

³ School of Automation, Harbin University of Science and Technology, Harbin 150080, China

* Correspondence: woo@hrbust.edu.cn; Tel.: +86-131-5980-2198

Abstract: In terms of the dynamic changes of battery model parameters in a single-model filtering algorithm, the filter estimation accuracy can be poor, and filtering is scattered due to the different internal state parameters of lithium-ion batteries in different aging states, which affects the state of charge (SOC). In order to address these issues, an Interacting Multiple Model (IMM) algorithm was proposed in this study, which adopted an Unscented Kalman Filter (UKF) to better approximate the nonlinear characteristics of the state equation while better stabilizing the filter and having lower computational requirements. Accordingly, the IMM was used to solve the problem of the accurate estimation of the SOC under the dynamic change of model parameters. Moreover, an electrochemical impedance spectrum was used to establish the electrochemical model, after which the lithium-ion equivalent electrochemical circuit model was established, which improved the complexity problem due to its high accuracy but complicated the calculation of the multi-order equivalent circuit model. By conducting experiments and simulations, the algorithm of IMM-UKF was shown to achieve an effective estimation of the battery SOC, even when the state parameters of lithium-ion batteries were uncertain.

Keywords: charge state estimation; electrochemical impedance spectrum; interactive multi-model; traceless Kalman filter



Citation: Huang, C.; Wu, H.; Li, Z.; Li, R.; Sun, H. Interacting Multiple Model for Lithium-Ion Battery State of Charge Estimation Based on the Electrochemical Impedance Spectroscopy. *Electronics* **2023**, *12*, 808. <https://doi.org/10.3390/electronics12040808>

Academic Editor: Fabio Corti

Received: 9 January 2023

Revised: 29 January 2023

Accepted: 30 January 2023

Published: 6 February 2023



Copyright: © 2023 by the authors. Licensee MDPI, Basel, Switzerland. This article is an open access article distributed under the terms and conditions of the Creative Commons Attribution (CC BY) license (<https://creativecommons.org/licenses/by/4.0/>).

1. Introduction

Lithium-ion batteries have been widely used in many applications, such as electric vehicles, portable devices, and so forth. Compared with traditional batteries, lithium-ion batteries have a larger capacity, higher safety performance, and a longer service life [1]. The state of charge (SOC) has been one of the most basic and important functions in the Battery Management System (BMS), playing a decisive role in battery performance and safety, while enabling the battery power and usage to be ascertained more quickly and clearly. Accordingly, how to effectively estimate the power battery charge state is a very important issue, which can help ensure the efficient and safe operation of power batteries [2].

Traditional SOC estimation methods are mainly divided into the ampere–time integration method, open-circuit voltage method, data-driven method, and the model method [3]. When using the ampere–time integration method, it is difficult to obtain the initial value of the SOC, which may easily form cumulative errors and is not suitable for working conditions [4]. The open-circuit voltage method requires the battery to be resting and in equilibrium, which is not suitable for online measurement of the SOC [5]. The data-driven method requires a large amount of training data, and estimation accuracy is greatly influenced by the training sample and method [6]. Meanwhile, the modeling method considers

the battery as a system, achieving the identification of the state space by modeling and estimating the lithium-ion battery SOC by carrying out discrete recursion of the state space. According to the different methods of parameters, identification can be divided into two approaches: the time-domain equivalent circuit model and frequency-domain equivalent circuit model [7]. Among them, the time-domain equivalent circuit model is divided into the internal resistance model (Rint model), the Davinan equivalent circuit model (Thevenin model), and the multi-order Resistor-Capacitance (RC) model. However, the time-domain equivalent circuit model has certain problems, such as low accuracy, unsuitability for long time simulation, and having complex models [5]. The frequency-domain equivalent circuit model, which is also known as the electrochemical impedance model, is an adaptive model that is based on the electrochemical kinetic characteristics of a lithium-ion battery system. This is characterized by the electrochemical impedance spectroscopy (EIS) in order to correspond to circuit elements, which encompasses the electrochemical model and the time-domain equivalent circuit model. The electrochemical impedance spectroscopy (EIS) is a nondestructive parameter measurement and an effective method for determining the dynamic behavior of the battery. The measurement of the EIS of the battery can be divided into an online and offline measurement. The online measurement method mainly applies a small amplitude sine wave voltage to the lithium-ion battery through the BMS, so that the battery system produces a sine wave current response. The change of the ratio of the excitation voltage to the response current is the impedance spectrum of the electrochemical system. The offline measurement method uses a professional electrochemical impedance meter to measure the battery impedance spectrum, which requires offline measurements and has a high detection accuracy. The electrochemical impedance spectrum (EIS) is able to clearly reflect the characteristics of the batteries' spectrum, and thus, analyzes the dynamic characteristics and kinetic processes inside the battery.

According to the literature [8], the relationship between the SOC and the impedance phase with temperature has been established using the battery impedance phase at a specific frequency as the SOC estimation parameter combined with a linear fitting algorithm. Accordingly, it has shown to provide a novel perspective for the SOC estimation of lithium iron phosphate batteries and can provide a theoretical basis for the application of EIS-based SOC estimation algorithms in vehicles. However, the study had errors in the temperature measurement, which led to large errors in the SOC estimation. In another study [9], parameters in the second-order RC equivalent circuit model were identified using offline parameter identification and online parameter identification with recursive least squares and a forgetting factor, respectively. Moreover, the extended Kalman filter method was used to achieve the estimation of a batteries' SOC. However, it did not take into account the effects of the external temperature and noise variations in the EKF algorithm on the SOC estimation during the estimation. One study [10] developed and trained a neural network model to estimate the state of charge of the battery using the results of the batteries' discharge current and electrochemical impedance spectrum. However, its estimation accuracy was dependent on the number of neurons in the hidden layer. Moreover, this method attained an estimation of the SOC solely based on a single neural network, without considering the problem of dynamic changes of the battery parameters due to aging during the whole life-cycle of the battery. The parameters of the model change according to the usage conditions (different aging degrees and working conditions).

In order to solve the bottleneck of a single electrochemical impedance spectrum model algorithm in the SOC estimation, the Interacting Multiple Model (IMM) algorithm can better describe the system's uncertainty caused by dynamic changes in the model parameters. In addition, the model can be added, subtracted, or changed at any time according to the actual situation, with a strong adaptive variable structure capability. Currently, IMM has been used in battery SOC estimation, and [11] two different parameters of the Davinan equivalent circuit have been used to describe the dynamic characteristics of lithium-ion batteries, which then utilized IMM-EKF and traditional EKF for a battery SOC estimation. The corresponding results demonstrated that the accuracy of the SOC values estimated based

on the IMM-EKF algorithm is much higher than that of traditional EKF. Another study [12] employed IMM combined with the Unscented Kalman Filter (UKF) and applied a genetic algorithm in order to optimize the battery model with different parameter space states for the battery SOC estimation, whose results were found to be more accurate. Additionally, another study [13] showed that for issues pertaining to when a single-model cannot capture the dynamic changes of the battery at different temperatures, a joint algorithm of IMM and the Square Root Unscented Kalman Filter (SRUKF) was used to achieve an accurate estimation of the battery SOC at different temperatures based on the first-order Davinan equivalent circuit. One study [14] also demonstrated that the parameters of the second-order RC battery equivalent model can be identified online using the recursive least squares method with a forgetting factor, in which the identified parameters were simulated jointly with the IMM-UKF algorithm to achieve an accurate estimation of the battery SOC at different discharge multipliers. Moreover, in [15], the parameters of the stable fusion model have also been determined based on the assumption of a normal distribution, for which the Proportional-integral observer (PIO) and Proportional-integral-differential observer (PIDO) fusion models jointly estimated the battery SOC, showing that the estimation results were more accurate and noise-resistant under different aging width temperatures. In a separate study [16], a first-order RC equivalent circuit model combined with the Preisach discrete model was established, where the FRISCH scheme was used to estimate and filter noise. Finally, the extended Kalman filter combined with the traceless Kalman filter was used to achieve real-time parameter updates and an accurate estimation of the batteries' single SOC. The aforementioned results show that the accuracy and robustness of the battery SOC estimation can be improved to a certain extent by using the traditional IMM model combined with an improved algorithm of Kalman filter.

In summary, this paper proposes an IMM filtering algorithm based on the electrochemical impedance spectrum and combines it with UKF to achieve the accurate estimation of the Li-ion battery. As previously mentioned, this is done in order to address issues in which the single-model filtering algorithm has to deal with dynamic changes of the parameters of the equivalent circuit model of the battery, which can result in a poor single-model filtering accuracy and a difficult filtering divergence due to the different states of the Li-ion battery under various aging conditions of the equivalent circuit model, thereby affecting the SOC estimation accuracy. UKF can estimate the charge state statistics of a Li-ion battery in real time by introducing a Markov chain state transfer probability matrix. Moreover, it can be combined with the electrochemical impedance spectrum model in the frequency domain so as to reflect the internal dynamic characteristics of a Li-ion battery accurately and intuitively. A filtering algorithm using UKF may also be able to better approximate the nonlinear characteristics of the SOC estimation with moderate computational effort. Accordingly, the final experiments and simulations show that the IMM-UKF algorithm can achieve an effective estimation of the battery SOC while improving the convergence speed of the filtering algorithm and ensuring the accuracy of the SOC estimation, even when the state parameters of the lithium-ion battery are uncertain.

2. Battery Electrochemical Impedance Spectrum Circuit Model and Parameter Identification

The battery model can be used to study the external characteristics of the battery during operation, which also serves as the basis for the battery SOC estimation. Battery models are mainly divided into equivalent circuit models and data-driven models [17]. Data-driven models based on data require a large amount of experimental data and are extremely dependent on network parameter selections and training sample accuracy. In addition, the training method can also have a significant impact on the errors. The time-domain equivalent circuit model in the equivalent circuit model cannot systematically reflect the operating characteristics of the battery electrode interface. Furthermore, the higher the cell order, the greater the complexity of the model [18]. The frequency domain equivalent circuit in the electrochemical impedance spectrum equivalent circuit modeling

method does not appear in the measurement of the polarization phenomenon caused by the perturbation signal. This occurs in order to ensure the linear relationship between the potential and current so that the electrode works in a quasi-steady state, thereby simplifying the measurement results. Moreover, as the electrochemical impedance spectrum can reflect more information about the electrode process kinetics and electrode interface structure [19], it can be used to analyze the battery performance. Thus, this study adopted the electrochemical impedance spectrum model to estimate the battery SOC.

2.1. Equivalent Circuit Model of Electrochemical Impedance Spectrum

In order to improve the accuracy of the electrochemical impedance spectrum equivalent circuit model for Li-ion batteries, it is first necessary to have an understanding of the basic characteristics of the electrochemical impedance spectrum, as shown in Figure 1. Here, the 1400 mAH lithium iron phosphate 18,650 lithium-ion battery electrochemical impedance spectrum used in the present study is shown, which consists of a circular arc and sloping line, where the arc reflects the polarization of the lithium-ion battery while the sloping line reflects the ion diffusion of the electrode reaction of the lithium-ion battery. An accurate electrochemical impedance spectrum equivalent circuit model should have a reasonable description of both processes.

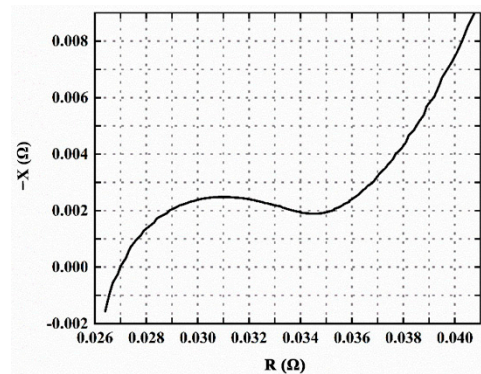


Figure 1. 18,650 LiFePO4 Li-ion battery electrochemical impedance spectrum.

An RC parallel circuit was used to fit the semicircular arc image in the electrochemical impedance spectrum, as shown in Figure 2.

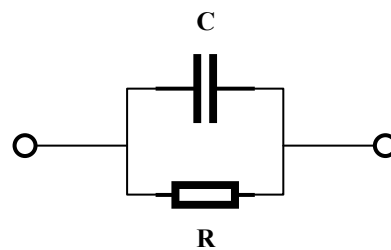


Figure 2. RC parallel circuit.

Combined with the significance of the parameters of the resistive and capacitive elements in the equivalent circuit of the electrochemical impedance spectrum, as shown in Equations (1) and (2), the total impedance of the parallel circuit is expressed in Equation (3), while the real impedance Z_{Re} and imaginary impedance Z_{Im} of the parallel circuit can be obtained, as shown in Equations (4) and (5), respectively. Accordingly, the relationship between the two is shown in Equation (6).

$$Z(j\omega) = R \tag{1}$$

$$Z(j\omega) = \frac{1}{j\omega C} \tag{2}$$

$$Z(j\omega) = \frac{1}{\frac{1}{R} + j\omega C} = \frac{1}{1 + j\omega CR} \tag{3}$$

$$Z_{Re} = \frac{R}{1 + \omega^2 C^2 R^2} \tag{4}$$

$$Z_{Im} = \frac{\omega CR^2}{1 + \omega^2 C^2 R^2} \tag{5}$$

$$\left(Z_{Re} - \frac{R}{2} \right)^2 + Z_{Im}^2 = \left(\frac{R}{2} \right)^2 \tag{6}$$

According to Figure 1, the electrochemical impedance spectrum of the lithium-ion battery intersected with the real axis, demonstrating a resistance where the resistance magnitude was the value of the real axis. Additionally, a semicircular arc can be equated to the RC parallel equivalent circuit, where the diameter of the semicircular arc was the resistance value of R in the RC circuit. The last straight line with a slope close to 45° was equated using Weber impedance. As a result, the equivalent circuit model of the electrochemical impedance spectrum of the experimental Li-ion battery was approximated, as shown in Figure 3.

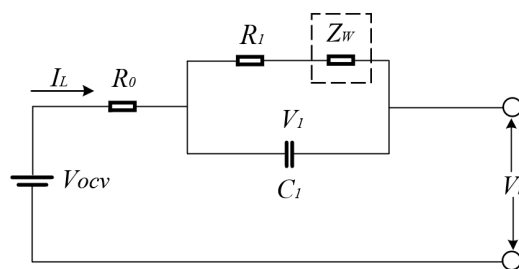


Figure 3. Electrochemical impedance spectrum equivalent circuit diagram.

In Figure 3, V_{ocv} is the open-circuit voltage of the battery; R_0 is the ohmic internal resistance of the battery; R_1 characterizes the internal charge transfer resistance of the battery; C_1 characterizes the capacitance due to the internal charge transfer of the battery; V_t is the terminal voltage of the battery; I_L is the charging or discharging current of the battery; and Z_W is the Warburg impedance.

In this figure, Z_W is the Warburg impedance (Warburg), which represents the impedance caused by the charge diffusion process. It is an important characteristic to evaluate the internal performance of the lithium-ion battery. When the impedance data are close to one, it indicates that the internal characteristics of the battery are better than others. However, the Warburg impedance has less influence on the charge transfer process than the charge transfer impedance and the ohmic impedance. Therefore, when the equivalent circuit model of the electrochemical impedance spectrum is combined with the traditional equivalent circuit model, the equivalent circuit element Z_W that represents the Warburg impedance can be ignored.

2.2. Electrochemical Impedance Spectrum Equivalent Circuit Model Parameter Identification Method

The fitting of the frequency response curve of the electrochemical impedance spectrum is an important issue in EIS data processing. It can be fitted using the electrochemical impedance spectrum fitting software ZSimpWin (version 3.5, Echem Software, Ann Arbor, MI, USA). Since the electrochemical impedance spectrum examines the nonlinear relationship between impedance and frequency, the software utilized the nonlinear least squares method to correlate the electrochemical impedance spectrum of lithium-ion batteries [20].

The angular frequency ω , as well as m , and the reference variables C_1, C_2, C_3, \dots , and C_m were used to represent the impedance G , as shown in Equation (7), where $G'(\omega, C_k)$ and $G''(\omega, C_k)$ represent the real and imaginary parts of the electrochemical impedance spectrum, denoting an impedance.

$$G = G(\omega, G_k) = G'(\omega, C_k) + jG''(\omega, C_k), k = 1, 2, 3, \dots, m \tag{7}$$

The least-squares fit of the electrochemical impedance spectrum sought to find the best estimate of the m parameters and minimize the sum of squares of the vector differences between the measured and calculated impedance values S . S can then be expressed by Equation (8).

$$S = \sum_{i=1}^n (q_i - G_i)^2 = \sum_{i=1}^n (q'_i - G'_i)^2 + \sum_{i=1}^n (q''_i - G''_i)^2, n > m \tag{8}$$

The difference between the initial value and best estimate Δk was initially solved, after which the parameters were determined. According to the conditions when solving the optimal solution of S , one can linearize S and build a system of equations for Δk , as shown in Equation (9), where the coefficients a_{ki} and b_k in the system of equations are shown in Equations (10) and (11), respectively.

$$\begin{aligned} a_{11}\Delta_1 + a_{12}\Delta_2 + a_{13}\Delta_3 + \dots + a_{1m}\Delta_m &= b_1 \\ a_{21}\Delta_1 + a_{22}\Delta_2 + a_{23}\Delta_3 + \dots + a_{2m}\Delta_m &= b_2 \\ a_{31}\Delta_1 + a_{32}\Delta_2 + a_{33}\Delta_3 + \dots + a_{3m}\Delta_m &= b_3 \\ a_{m1}\Delta_1 + a_{m2}\Delta_2 + a_{m3}\Delta_3 + \dots + a_{mm}\Delta_m &= b_m \end{aligned} \tag{9}$$

$$a_{ki} = \sum_{i=1}^n \left(\frac{\partial G'_i{}^0}{\partial C_k} \frac{\partial G_i^0}{\partial C_i} + \frac{\partial G''_i{}^0}{\partial C_k} \frac{\partial G_i^0}{\partial C_i} \right) \tag{10}$$

$$b_k = \sum_{i=1}^n \left[(g'_i - G_i^0) \frac{\partial G_i^0}{\partial C_k} + (g''_i - G_i^0) \frac{\partial G_i^0}{\partial C_k} \right] \tag{11}$$

As per the system data measured in Figure 3 and by setting the initial values of the parameters, the difference in Δk between the coefficients and the initial values in the impedance expression as well as the optimal estimate were obtained. The C_k estimate was then obtained by substituting Δk into the complex function equation, as shown in Equation (12).

$$C_k = C_k^0 + \Delta k, k = 1, 2, \dots, m \tag{12}$$

This fitting method gradually reduced the deviation Δk between the initial value of the parameter and the best estimate by iterating continuously in order for the estimated parameter value using this method to be closer to the true value. When Δk was too small to be ignored, the current estimated value was considered to be approximately equal to the true value.

2.3. Verification Based on the Accuracy of the Electrochemical Impedance Spectroscopy Model

As shown in Figure 4, a 1400 mAh LiFePO4 18,650 battery was used to the experimental object and selected the equivalent circuit model of the electrochemical impedance spectrum to fit the curve. It can be calculated from the figure that the error of the electrochemical impedance spectrum equivalent circuit model is 1.29%.

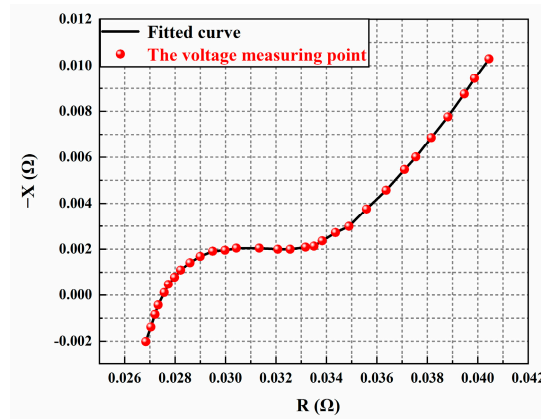


Figure 4. Electrochemical impedance spectrum fitting curve.

3. Interactive Multi-Model Algorithm Based on the Electrochemical Impedance Spectrum Model

Suppose the battery had r SOC estimation models, which can be described by a set, i.e., $\{m_1, m_2, m_3, \dots, m_r\}$, where the system equation of state and measurement equation of the j th model is:

$$\begin{aligned} X_k^j &= f_{k-1}^j(X_{k-1}^j, \Phi_{k-1}) + W_{k-1}^j = A_{k-1}^j X_{k-1}^j + B_{k-1}^j \Phi_{k-1} + w_{k-1}^j, j = 1, 2, 3, \dots, n \\ Z_k &= h_k^j(X_k^j, \Phi_k) + v_k = C_k^j X_k^j + v_k \end{aligned} \tag{13}$$

where X_k^j is the state variable of the system, Z_k is the observed variable of the system, f and h are nonlinear functions, respectively, W_k^j is the process noise matrix of the system, and v_k^j is the measurement noise matrix of the system, and both conform to the Gaussian distribution with variances Q_k^j and R_k^j , respectively, and both are known. Meanwhile, each model contained a separate UKF to track its state, in which the probability of each model was adjusted in real time using the hidden Markov chain. In order to improve the adaptive and self-learning capability of the algorithm, an unsupervised learning method was used to estimate the parameters of the hidden Markov model and establish a time-varying hidden Markov probability transfer matrix that can be corrected in real time, which was adopted the BaumWelch algorithm and the estimated probability transfer matrix p_{ij} as [21].

$$p_{ij} = \frac{\sum_{t=1}^{k-1} \zeta_t^{ij}}{\sum_{t=1}^{k-1} \gamma_t^i} \tag{14}$$

γ_t^i is the probability of the model at the time, and ζ_t^{ij} is the probability that the model was transferred from, at the time. To ensure the accuracy and real time nature of the model, the probability transfer matrix at the time was used as the current transfer probability.

In Figure 3, the Warburg impedance could not be easily measured due to its variation with frequency. Moreover, the resistance value was too small when compared with the resistance to be negligible. As seen in Figure 3, the electrochemical impedance spectrum equivalent circuit yielded the cell terminal voltage V_t as:

$$V_t = I_L R_0 + V_1 + V_{OCV} \tag{15}$$

V_1 and I_L are positive when charging and negative when discharging.

The voltages across capacitor C_1 are:

$$\dot{V}_1 = -\frac{V_1}{R_1 C_1} + \frac{I_L}{C_1} \tag{16}$$

SOC can be calculated as:

$$SOC = SOC(0) - \frac{\eta}{Q_r} \int_0^\tau I_L(t) d(t) \tag{17}$$

where $SOC(0)$ is the initial state of SOC, η is the Coulomb efficiency, and Q_r is the rated capacity of the battery.

The open-circuit voltage V_{ocv} of the battery was basically equal to the electric potential of the battery, which is an important parameter that characterizes the energy of the battery. In addition, a functional relationship exists with the batteries' state of charge (state of charge, SOC), which can be expressed as:

$$V_{ocv} = f(SOC) \tag{18}$$

This study used the constant current discharge method in order to fit the equation of the 9th order matrix to V_{ocv} and SOC as:

$$V_{ocv} = a_0 + a_1 SOC^9 + a_2 SOC^8 + a_3 SOC^7 + a_4 SOC^6 + a_5 SOC^5 + a_6 SOC^4 + a_7 SOC^3 + a_8 SOC^2 + a_9 SOC \tag{19}$$

The obtained $V_{ocv} - SOC$ curve can be shown in Figure 5 [22]:

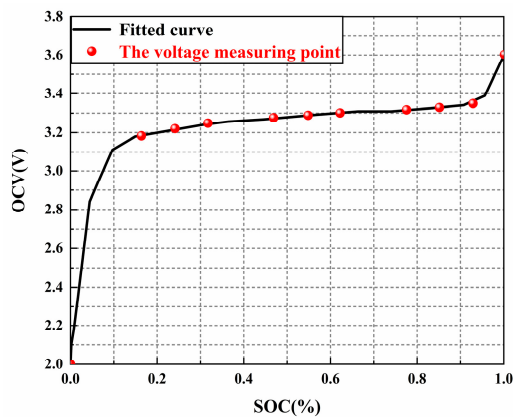


Figure 5. $V_{ocv} - SOC$ fitting curve [22].

Combining the discrete forms of (15), (16), and (17), the battery state equation and measurement equation can be obtained as:

$$\begin{bmatrix} SOC_k \\ V_{1,k} \end{bmatrix} = \begin{bmatrix} 1 & 0 \\ 0 & e^{-T/\tau_1} \end{bmatrix} \times \begin{bmatrix} SOC_{k-1} \\ V_{1,k-1} \end{bmatrix} + \begin{bmatrix} -\eta T / Q_r \\ R_1 (1 - e^{-T/\tau_1}) \end{bmatrix} \times I_{L,k} + \begin{bmatrix} w_{1,k} \\ w_{2,k} \end{bmatrix} \tag{20}$$

$$V_{t,k} = \begin{bmatrix} \frac{V_{ocv} - I_{L,k} R}{SOC_k} & -1 \end{bmatrix} \times \begin{bmatrix} SOC_k \\ V_{1,k} \end{bmatrix} + v_k \tag{21}$$

where $\tau_1 = R_1 C_1$, $V_{ocv} = f(SOC_k)$.

The state variable is $X_k = [SOC_k \ V_{1,k}]$, the control variable is $I_{L,k}$, and the measurement variable is $V_{t,k}$.

In summary, and combined with the electrochemical impedance spectrum equivalent circuit model in Section 2, the equation of state and the observation equation matrix coefficients of the cell for any first model are thus:

$$A_{k-1}^j = \begin{bmatrix} 1 & 0 \\ 0 & e^{-T/\tau_1^j} \end{bmatrix}, B_{k-1}^j = \begin{bmatrix} -\eta T / Q_\gamma \\ R_1^j (1 - e^{-T/\tau_1^j}) \end{bmatrix}, C_k^j = \begin{bmatrix} \frac{V_{OCV} - I_{L,k} R}{SOC_k} & -1 \end{bmatrix} \quad (22)$$

Comparing Equation (14), the coefficients A_k^j , B_k^j , C_k^j , and X_k^j of the equation were then determined, after which the estimated value of the SOC was calculated.

During the initialization of the equations, the initialization parameters included the state transfer probability matrix p in the IMM, the probability matrix μ of the model, coefficients A, B, C , the covariance matrix of the state, and the measurement equations, which were incorporated into the SOC estimation algorithm of IMM-UKF.

The overall flowchart is shown in the following Figure 6.

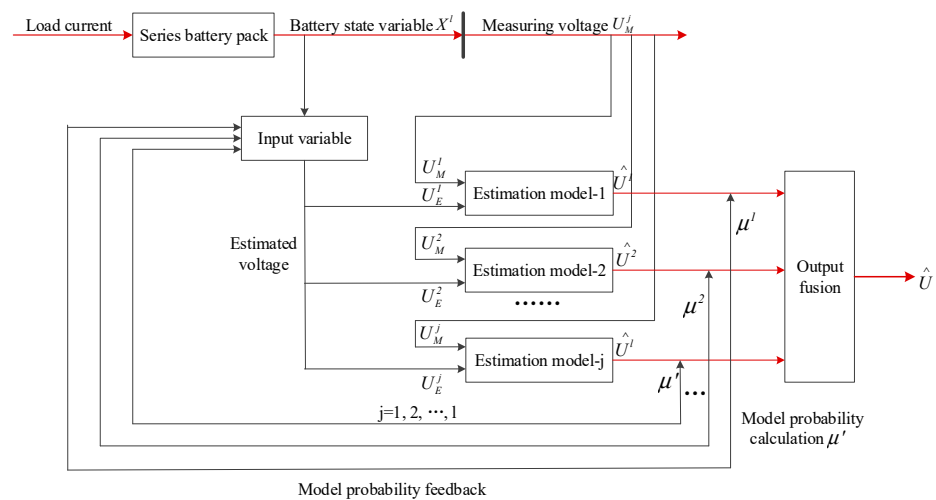


Figure 6. Overall flow chart.

According to Figure 6, the parameters of the n models were first separately identified, after which the associated state equations were initialized. The initial interaction of the individual fault model information based on the IMM was then performed so that each model probability was updated at each cycle. The UKF filter estimator of each model estimated and corrected the posterior unknown process and measurement noises in real time, in order to adapt to the current environment while enhancing the convergence speed of the model. Additionally, the UKF was filtered so as to obtain the optimal estimate of the current lithium-ion battery SOC. Finally, the updated model probability was fed back to the input for the input to fuse the historical information of the output and reduce the complexity of the optimal estimation method.

4. Experimental Study Based on Interactive Multi-Model SOC Estimation Model

Three kinds of experimental platforms were used: the Arbin BT-ML-30 V/10 A power battery tester produced by Arbin USA, ZM3000E; the battery internal resistance tester produced by Harbin Zeemoo Technology Co., Ltd.; and the CHI650D electrochemical workstation produced by Shanghai Chenhua Instrument Co. This study used different batteries in the Arbin experimental platform cycle aging test. The voltage measurement range of the Arbin equipment was 0–30 V; the current measurement range was 0–10 A; and the resolution of voltage and current measurement were able to reach 0.1 mV and 0.1 mA, respectively. Meanwhile, the voltage scan range of CHI650D was 0.05–3 V, and the scan rate was 0.5 mV/s. The specific experimental platform is shown in Figure 7.

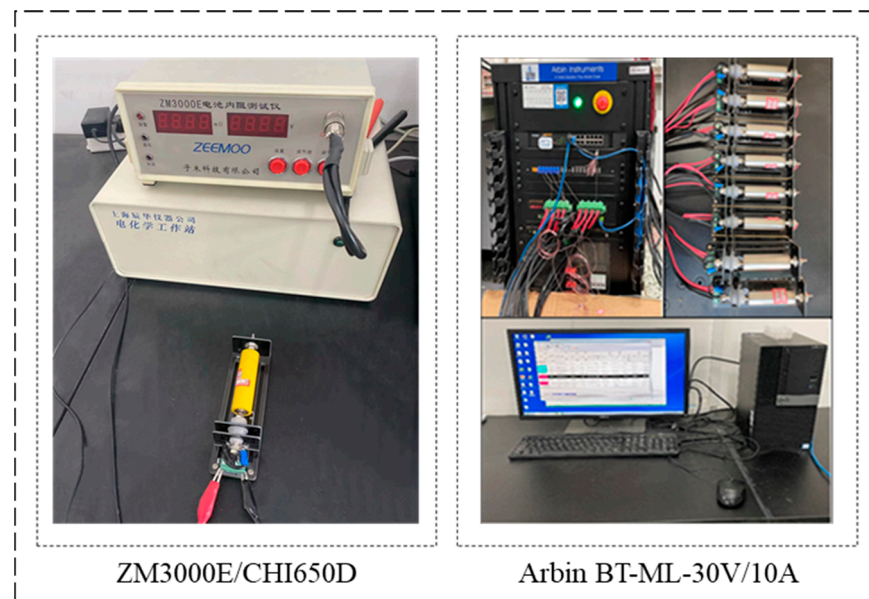


Figure 7. Battery experimental platform.

The experimental battery was a 18,650-type lithium-ion phosphate battery with a nominal capacity of 1.4 Ah. In order to obtain a lithium-ion battery with different model parameters, this study adopted the cycling test method in FreedomCar to cycle the battery for aging. The new battery, the battery with 300 cyclings, and the battery with 500 cyclings were then taken as the objects of the study, after which the batteries were discharged at a constant current with a discharge multiplier of 1C for the three cycling states. The discharge curves for the three cycling times are shown in Figure 8 [23].

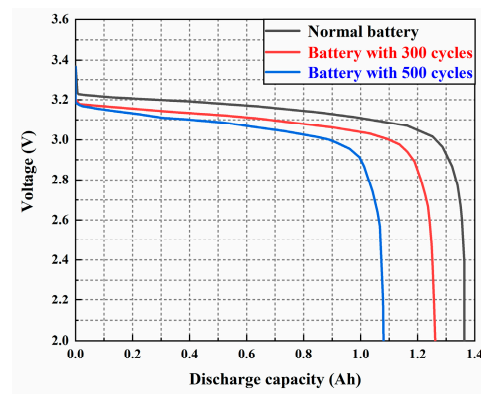


Figure 8. Discharge curve of the battery under three cycle times [23].

As shown in Figure 8, as the number of battery cycles rose, the discharge plateau of the battery became increasingly lower, the discharge capacity became smaller, and the battery health (state of health, SOH) reduced. Table 1 shows the battery capacity and SOH values for the three cycling states. The models for the three cycling times were abbreviated as Model 1, Model 2 and Model 3, which are shown in Table 1.

Table 1. Battery capacity and SOH values for the three cycle states.

Model	Number of Cycles	Capacity (mAh)	SOH (%)
1	0	1400	100
2	300	1278	91.3
3	500	1095	78.2

The resistance and capacitance parameters were identified for the three batteries under SOH using the electrochemical impedance spectra, as shown in Figure 9. Moreover, the identification method was that as described in Section 2.2, and the specific parameter values were obtained, as shown in Table 2. According to Figure 9, the electrochemical impedance spectra of the Li-ion battery shifted to the right with a rise in the number of cycles, indicating that the rise in cycles of the Li-ion battery increased its ohmic internal resistance and polarization resistance. As a result, three different models of lithium-ion batteries for the SOC estimation were obtained.

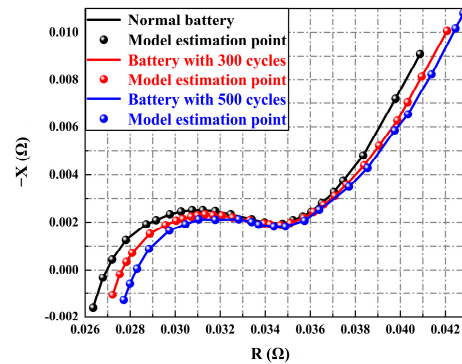


Figure 9. Electrochemical impedance spectrum curves of the battery at three cycle counts.

Table 2. Values of resistance and capacitance parameters at different SOH.

Model	R_0 (Ω)	R_1 (Ω)	C_1 (F)
1	0.0263	0.0042	0.1977
2	0.0275	0.0069	0.1696
3	0.0281	0.0095	0.1468

From Table 2, as the number of cycles rose, the internal resistance parameter of the battery was shown to increase while the capacitance parameter decreased; hence, the equivalent model of the battery also changed dynamically.

Based on the above three resistance–capacitance parameter models, the IMM-UKF algorithm was used in order to establish the corresponding three battery equivalent models. The highest matching degree demonstrated that the model was the current actual operating model.

The power demand value was then scaled down to the allowable output power of a single battery, and the fully charged battery ($SOC = 1$) was then placed in a 25 °C thermostat and left for 2 h. A programmable DC electronic load was used to simulate the above demanded power sequence, of which the power of the programmable load was set to “1” when the battery was discharged under working conditions. The battery discharge current, terminal voltage, and battery SOC are shown in Figure 10.

The calculation results using a single-model and multi-model are shown in Figure 11. The curve is the SOC estimation diagram of the sample battery in 238 cyclings. A comparison of the three single-model and multi-model estimates is shown in Figure 11a, in which the estimated value of Model 3 better matched the true SOC value, while the estimated values of Model 1 and Model 2 did not match the true SOC value that well. Therefore, the three Model 3 estimates, the multi-model estimates, and the true SOC were then compared, as shown in Figure 11b, where the majority of the blue boxes were enlarged.

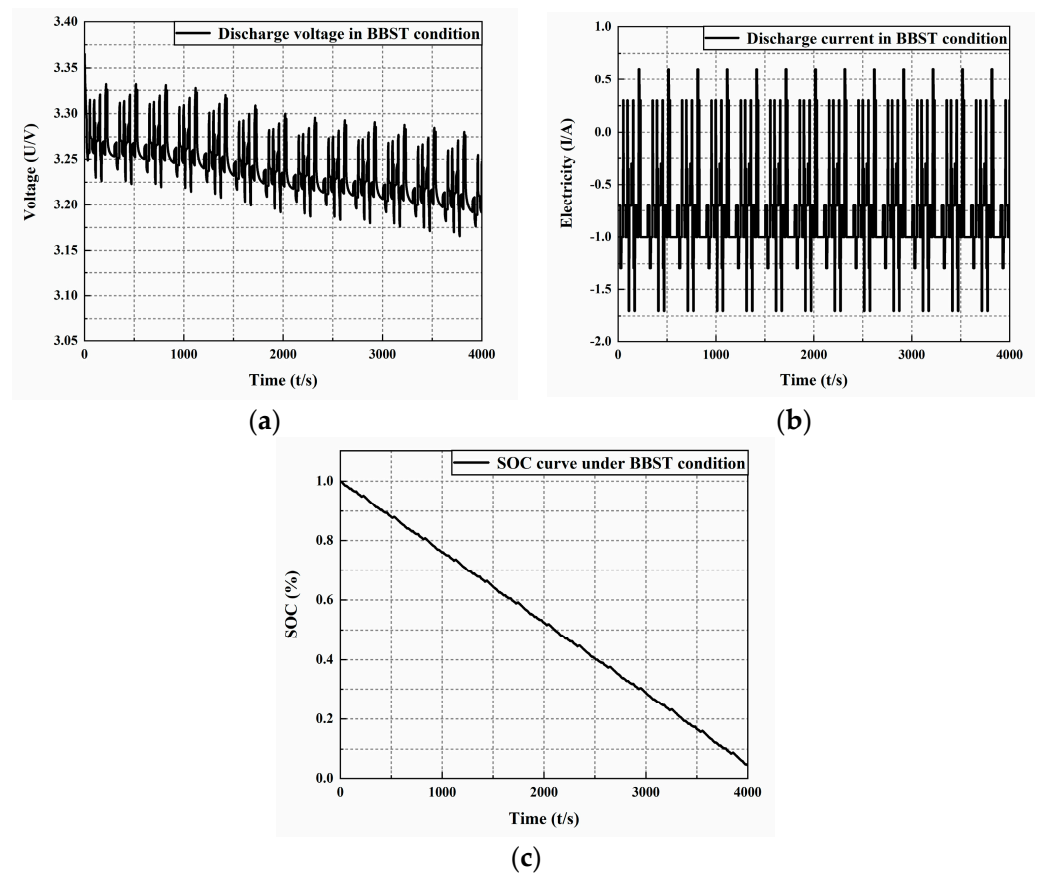


Figure 10. Battery discharge current, terminal voltage, and SOC under BBST conditions. (a) Battery discharge current under BBST conditions. (b) Battery terminal voltage under BBST conditions. (c) Battery SOC under BBST conditions.

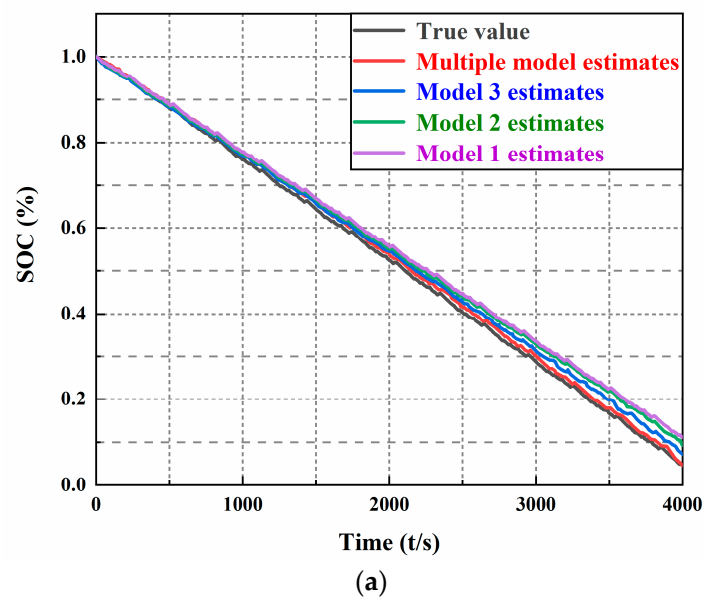


Figure 11. Cont.

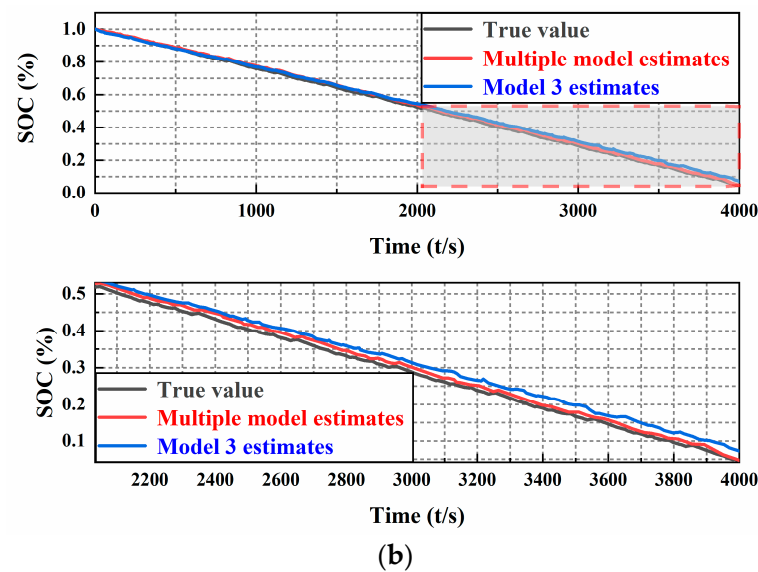


Figure 11. SOC estimation results. (a) SOC estimation curves of multi-model and each single-model. (b) SOC estimation curves of multi-model and Model 3.

The multi-model estimation results in SOC estimation in Figure 11 was found to be similar to the real SOC values, demonstrating that the algorithm can accurately and effectively accomplish the SOC estimation for Li-ion batteries when the parameters dynamically change under multiple models.

Meanwhile, the results of the multi-model estimation were noted to be gradually close to overlapping with those of Model 3, indicating that the weights of Model 3 were gradually close to one in multi-model estimation. Meanwhile, the gradual deviation of Model 1 and Model 2 from the multi-model estimation indicated that the weights of Model 1 and Model 2 were gradually close to zero in multi-model estimation. Figure 12 shows the conditional probabilities of the three models.

Based on the above analysis of the multi-model and single-model SOC estimation, the conditional probabilities of Model 1 and Model 2 were shown to rapidly drop to 0 within 100 s after the start of the operation, while the conditional probability of Model 3 rapidly climbed to 0.95 within the same time. A further analysis was performed using the multi-model and single-model SOC estimation errors, as illustrated in Figure 13.

As seen in Figure 13, regarding the three single-model SOC estimation and the multi-model estimation errors, the estimation error of the SOC using the traceless Kalman filter of Model 1 and Model 2 was larger, while using the multi-model traceless Kalman filter algorithm reduced the error and increased accuracy, thereby improving the robustness of the system. Meanwhile, the maximum estimation error of Model 1 was found to be 28.9%, while the maximum estimation error of Model 2 was 6.5%, which was larger than the real SOC value. In addition, the maximum estimation error of Model 3, which was observed to be similar to the multi-model estimation, was 1%. The multi-model estimation had an error of less than 1% due to the integration of information from multiple aging cells, which was the smallest method among the three single-model SOC estimation errors.

According to the comparison, the estimation error of the UKF algorithm was noted to be much larger than that of the IMM-UKF algorithm, demonstrating that the average error was three times higher than that of the latter, with the maximum error also being 0.7% higher. This caused UKF to be in a divergent state for the vast majority of the filtering time, thus affecting the estimation accuracy of the overall SOC. In contrast, IMM-UKF had minimal limitations in estimating the SOC of different Li-ion batteries, with an average error only 0.08% higher and a maximum error 0.43% higher after fusing other aging batteries' information. Accordingly, this illustrates that the algorithm can guarantee the accuracy and validity of the SOC estimation of Li-ion battery states.

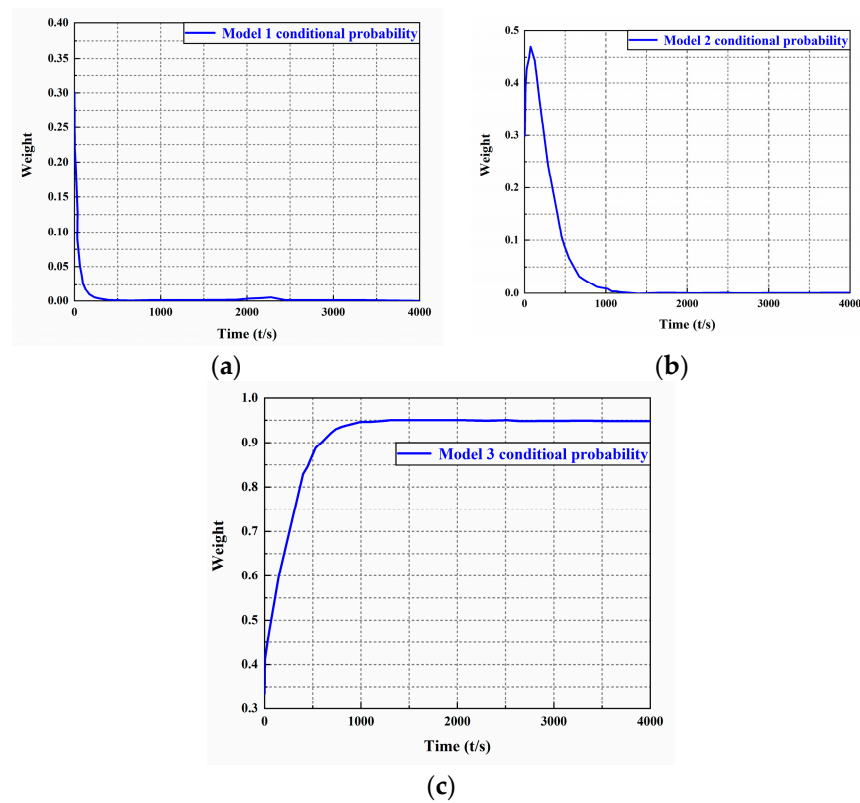


Figure 12. Weights curve of different battery models. (a) Weight curve of battery Model 1. (b) Weight curve of battery Model 2. (c) Weight curve of battery Model 3.

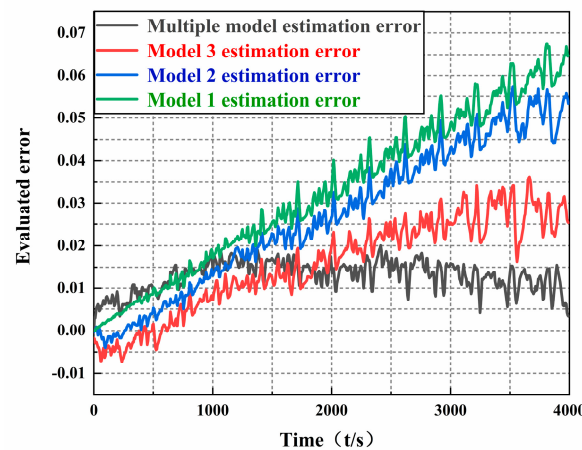


Figure 13. Multi-model and single-model SOC estimation errors.

5. Conclusions

This study presented a novel SOC estimation method for IMM-UKF batteries based on the electrochemical impedance spectrum equivalent circuit with an interactive multi-model algorithm, which was then combined with the traceless Kalman filter to achieve an accurate SOC estimation with dynamic changes in the model parameters. The electrochemical impedance spectrum equivalent circuit equates the internal lithium-ion battery via the impedance spectrum method, enabling the equivalent circuit to be more reflective of the lithium-ion battery electrode process while making it more accurate and reducing errors. As a result, this allows the entire UKF model set to be able to estimate a series of statistical information in real time and realize the regulation of posteriori unknown SOC information. The final experiments and simulations in this study demonstrated that IMM-UKF can

accomplish an SOC estimation under multiple models with an average error of less than 1% and a maximum error of only 1%. Meanwhile, compared with the SOC estimation results in the single-model case, the IMM-UKF algorithm combined multiple cell information with a significant decrease in both the average error and maximum error. Moreover, combined with the number of iterations, the convergence speed of the IMM-UKF algorithm was shown to be higher than that of the single-model UKF algorithm. Finally, when comparing Model 2 and IMM estimation, the weight value of the UKF algorithm in Model 2 was close to 0.95, with the single not reaching 1, which was far inferior to the IMM-UKF algorithm in the same state. The IMM-UKF algorithm can efficiently complete the SOC estimation of a lithium-ion battery with different state parameters, which ensures the accuracy and validity of the SOC estimation while improving convergence speed. Therefore, the findings of this study may provide a strong theoretical basis for lithium-ion batteries in SOC state estimation.

Author Contributions: Conceptualization, C.H. and H.W.; methodology C.H.; software, Z.L.; validation, C.H., H.W., R.L., Z.L. and H.S.; formal analysis, C.H. and Z.L.; investigation, C.H.; resources, C.H. and H.W.; data curation, C.H., R.L. and Z.L.; writing—original draft preparation, Z.L.; writing—review and editing, C.H., H.W. and Z.L.; visualization, C.H. and H.S.; supervision, C.H., H.W., R.L. and H.S.; project administration, C.H. and H.S.; funding acquisition, R.L. All authors have read and agreed to the published version of the manuscript.

Funding: This work was supported by “the Joint Fund Project of the Ministry of Education of China (8091B022133)” and “the Natural Science Foundation of Heilongjiang Province, China (Grant No. LH2022E08)”.

Conflicts of Interest: The authors declare no conflict of interest.

References

1. Li, J.; Liu, M. State-of-charge estimation of lithium-ion batteries using composite multi-dimensional features and a neural network. *IET Power Electron.* **2019**, *12*, 1470–1478. [\[CrossRef\]](#)
2. Trilla, L.; Casals, L.C. Dual Extended Kalman Filter for State of Charge Estimation of Lithium-Sulfur Batteries. *Energies* **2022**, *15*, 6989. [\[CrossRef\]](#)
3. Qaisar, S.M. A Proficient Li-Ion Battery State of Charge Estimation Based on Event-Driven Processing. *J. Electr. Eng. Technol.* **2020**, *15*, 1871–1877. [\[CrossRef\]](#)
4. Castanho, D.; Guerreiro, M. Method for SoC Estimation in Lithium-Ion Batteries Based on Multiple Linear Regression and Particle Swarm Optimization. *Energies* **2022**, *15*, 6881. [\[CrossRef\]](#)
5. Andre, D.; Appel, C. Advanced mathematical methods of SOC and SOH estimation for lithium-ion batteries. *J. Power Sources* **2013**, *224*, 20–27. [\[CrossRef\]](#)
6. Wu, T.; Chen, X. Research on SOC Hybrid Estimation Algorithm of Power Battery Based on EKF. In Proceedings of the Asia-Pacific Power and Energy Engineering Conference, Wuhan, China, 25–28 March 2011; p. 11.
7. Zhang, W.; Lei, G. Research on the equivalent circuit model of lithium-ion batteries. *Power Technol.* **2016**, *40*, 1135–1138.
8. Dai, H.; Wang, D. Battery charge state estimation based on electrochemical impedance spectroscopy. *J. Tongji Univ. Nat. Sci. Ed.* **2019**, *47*, 95–98.
9. Liu, C.; Zhang, Y. Identification of lithium-ion battery parameters and estimation of charge state. *Energy Storage Sci. Technol.* **2022**, *11*, 3618–3622.
10. Luo, Y.-F. A Multi-Frequency Electrical Impedance Spectroscopy Technique of Artificial Neural Network-Based for the Static State of Charge. *Energies* **2021**, *14*, 2526. [\[CrossRef\]](#)
11. Xia, X.; Wei, Y. Lithium-Ion Batteries State-of-Charge Estimation Based on Interactive Multiple-Model Extended Kalman Filter. In Proceedings of the 22nd International Conference on Automation and Computing, Colchester, UK, 7–8 September 2016; p. 204.
12. Peng, S.; Chen, C. State of Charge Estimation of Battery Energy Storage Systems Based on Adaptive Unscented Kalman Filter With a Noise Statistics Estimator. *IEEE Access* **2017**, *5*, 13202–13212. [\[CrossRef\]](#)
13. Ouyang, Q.; Ma, R. Adaptive Square-Root Unscented Kalman Filter-Based State-of-Charge Estimation for Lithium-Ion Batteries with Model Parameter Online Identification. *Energies* **2020**, *13*, 4968. [\[CrossRef\]](#)
14. Chen, D.; Wang, C. Interactive multi-model traceless Kalman filtering algorithm for predicting lithium battery SOC. *Energy Storage Sci. Technol.* **2020**, *9*, 257–265.
15. Xiong, R.; Ma, S. Toward a safer battery management system: A critical review on diagnosis and prognosis of battery short circuit. *iScience* **2020**, *23*, 101010. [\[CrossRef\]](#)
16. Liu, Z.; Li, P. Lithium battery parameter identification and SOC online joint estimation based on combined model. *China Mech. Eng.* **2020**, *31*, 1162–1168.

17. Estaller, J.; Kersten, A. Overview of Battery Impedance Modeling Including Detailed State-of-the Art Cylindrical 18650 Lithium-Ion Battery Cell Comparisons. *Energies* **2022**, *15*, 3822. [[CrossRef](#)]
18. Salazar, D.; Garcia, M. Estimation and Comparison of SOC in Batteries Used in Electromobility Using the Thevenin Model and Coulomb Ampere Counting. *Energies* **2022**, *15*, 7204. [[CrossRef](#)]
19. Tan, J.; Yan, X. Estimation of state-of-charge for lithium-ion battery by interactive multiple model Kalman filter. *Sci. Technol. Eng.* **2019**, *19*, 170–175.
20. Zhang, H. Parameter identification method for photovoltaic cells based on nonlinear least squares method. *Mod. Electr. Power* **2017**, *34*, 79–84.
21. Pan, S.; Hu, S. Prediction of power battery state of charge based on EKF-Markov. *Chin. J. Power Sources* **2016**, *40*, 990–993.
22. Wang, Y.; Meng, D. Multi-Fault Diagnosis of Interacting Multiple Model Batteries Based on Low Inertia Noise Reduction. *IEEE Access* **2021**, *9*, 18465–18480. [[CrossRef](#)]
23. Huang, C.; Yu, X. State of charge estimation of li-ion batteries based on the noise-adaptive interacting multiple model. *Energy Reports* **2021**, *7*, 8152–8161. [[CrossRef](#)]

Disclaimer/Publisher’s Note: The statements, opinions and data contained in all publications are solely those of the individual author(s) and contributor(s) and not of MDPI and/or the editor(s). MDPI and/or the editor(s) disclaim responsibility for any injury to people or property resulting from any ideas, methods, instructions or products referred to in the content.